Latin American Journal of Solids and Structures
www.lajss.org

Enhanced Biogeography-based Optimization: A New Method for Size and Shape Optimization of Truss Structures with Natural Frequency Constraints

Abstract

The current study presents an enhanced biogeography-based optimization (EBBO) algorithm for size and shape optimization of truss structures with natural frequency constraints. The BBO algorithm is one of the recently developed meta-heuristic algorithms inspired by the mathematical models in biogeography science and is based on the migration behavior of species among the habitats in the nature. In this study, the overall performance of the standard BBO algorithm is enhanced by new migration and mutation operators. The efficiency of the proposed algorithm is demonstrated by utilizing four benchmark truss design examples with frequency constraints. Numerical results show that the proposed EBBO algorithm not only significantly improves the performance of the standard BBO algorithm, but also finds competitive results compared with recently developed optimization methods.

Keywords

Biogeography-based optimization, meta-heuristic, truss structures, dynamic constraints, size and shape optimization.

Seyed Heja Seyed Taheri [a]
Shahin Jalili [b]

[a] Islamic Azad University, Urmia, Iran. Hejataheri@gmail.com

[b] Young Researchers and Elite Club, Urmia Branch, Islamic Azad University, Urmia, Iran. Shahinjalili@tabrizu.ac.ir

http://dx.doi.org/10.1590/1679-78252208

Received 11.06.2015
In revised form 13.03.2016
Accepted 16.03.2016
Available online 23.03.2016

1 INTRODUCTION

The ability to control and modify the values of free vibrational frequencies and corresponding mode shapes in structures is a significant issue to keep their vibrational performance desirable. In most of the low frequency vibration problems, the response of the structure to dynamic excitation is primarily a function of its fundamental frequency and mode shapes (Grandhi, 1993). Particularly, this is an important issue when a certain excitation frequency can cause resonance phenomena in the structure. Therefore, structural optimization with natural frequency constraints has important applications in manipulating the dynamic performance of the structures.

From optimization point-of-view, size optimization of truss structures with frequency constraints is described as highly non-linear and non-convex optimization problem with several local optimums in its search space. On the other hand, if the shape variables, beside the size variables, are considered to resolve this problem, the optimization problem will become more complex, and the associative performance will degrade seriously. The main reason for this complexity is related to the different physical representation of these variables, and sometimes their changes are of widely different orders of magnitude (Wang et al., 2004). Therefore, the size and shape optimization of truss structures with frequency constraints is one of the active areas in the research of structural optimization at present.

Generally, two main approaches are available in the literature to address the structural optimization problem with frequency constraints. These approaches are the conventional optimization techniques based on the use of classical gradient-based optimization techniques, and the meta-heuristic search methods based on the use of nature-inspired stochastic optimization algorithms. Nevertheless, the conventional methods such as the optimality criteria (OC) and mathematical programming (MP), need complex and time-consuming dynamic sensitivity analysis and are easily trapped into local optimum (Lingyun et al., 2005). On the other hand, the meta-heuristic search methods such as the genetic algorithms (GAs) (Goldberg, 1989), particle swarm optimization (PSO) (Eberhart and Kennedy, 1995), big bang-big crunch (BB-BC) algorithm (Erol and Eksin, 2006), gravitational search algorithm (GSA) (Rashedi et al., 2009), biogeography-based optimization (BBO) (Simon, 2008; Jalili et al., 2015), Cultural Algorithm (CA) (Reynolds, 1999; Jalili and Hosseinzadeh, 2015), and charged system search (CSS) algorithm (Kaveh and Talatahari, 2010) require less computational effort and can also find near-optimum solutions in a relatively reasonable time. Therefore, meta-heuristic optimization techniques are usually preferred to conventional approaches, and in most cases, show much better performances. However, it is widely believed that the overall performance of heuristic search methods mainly depends on the type of the optimization problem and the features of its search space. Hence, extensive studies have been carried out to develop efficient heuristic optimization methods for size and shape optimization of truss structures with natural frequency constraints, ranging from hybrid techniques to enhanced versions of standard algorithms. The Democratic PSO (DPSO) algorithm (Kaveh and Zolghadr, 2014a), hybrid CSS-BBBC algorithm (Kaveh and Zolghadr, 2012), enhanced CSS algorithm (Kaveh and Zolghadr, 2011), niche hybrid genetic algorithm (NHGA) (Lingyun et al., 2005), and orthogonal multi-gravitational search algorithm (OMGSA) (Khatibinia and Naseralavi, 2014) are some instances of these methods.

In this study, an enhanced biogeography-based optimization (EBBO) algorithm has been proposed to tackle the challenge of finding global optimum in size and shape optimization of truss structures with multiple frequency constraints. Biogeography-based optimization (BBO) is a recently developed population-based meta-heuristic algorithm based on the biogeography theory, which has been introduced by Simon (2008). The biogeography theory describes the geographical distribution of biological organisms in the nature. The BBO method is a successful meta-heuristic search technique that has been successfully applied to global optimization of numerical functions (Simon et al., 2011; Boussaid, 2012) and has been used to solve numerous real-world optimization problems (Simon, 2008; Singh e al., 2010; Bhattachary et al., 2010). However, despite having good exploitation ability, the standard BBO algorithm suffers from premature convergence; furthermore, its weak exploration ability is an issue in some cases. The main reason for this poor exploration ability arises from its simple

migration operator. In addition, the simple and purely random mutation operator of the BBO may lead to revisiting non-productive regions of the search space. In this study, in order to enhance the performance of standard BBO algorithm, new migration and mutation operators are proposed. These new migration and mutation operators improve the convergence properties of the BBO algorithm and enhance the algorithm's ability to further escape stagnation and premature convergence. To evaluate the efficiency of the proposed algorithm, four benchmark truss design examples with frequency constraints are investigated and the results generated by the EBBO algorithm are compared with the results of several other state-of-the-art methods. Numerical results show that the proposed EBBO algorithm not only significantly improves the standard BBO algorithm, but also finds competitive results compared with recently developed optimization methods for truss optimum design problem with frequency constraints.

The remaining sections complete the presentation of this paper as followings. Section 2 formulates the optimum design problem of truss structures with frequency constraints. In Section 3, the BBO algorithm is first reviewed and then, the proposed EBBO algorithm is explained in detail. Four benchmark truss design examples are optimized by utilizing the proposed algorithm in Section 4. Finally, the concluding remarks are presented in Section 5.

2 TRUSS OPTIMUM DESIGN PROBLEM

The main purpose of this optimum design problem is to minimize the weight of the structure under some frequency constraints. In the layout and size optimization of truss structures, the cross sectional areas and the coordinates of nodes are considered as design variables. Thus, the optimal design of a truss structure with frequency constraints can be formulated as:

$$\begin{gathered}\text{Find: } X = \{x_1, x_2, \dots, x_n\} \\ \text{To minimize: } \text{Cost}(\{X\}) = W(\{X\}).\, f_p(\{X\}) \\ W(\{X\}) = \sum_{i=1}^{m} \gamma A_i l_i \\ \text{Subjected to:} \\ C^U(\{X\}) = \frac{\omega_j}{\omega_j^u} - 1 \le 0 \\ C^L(\{X\}) = 1 - \frac{\omega_j}{\omega_j^l} \le 0 \\ L_k \le x_k \le U_k\end{gathered} \tag{1}$$

where $\{X\}$ is the vector including design variables; n is the number of the design variables; $W(.)$ is the weight of the structure; $f_p(.)$ is the penalty function; m is the number of structural members; γ is the material density; A_i and l_i are the cross-sectional area and length of member i, respectively; $C^U(.)$ and $C^L(.)$ are the upper and lower frequency constraints, respectively; ω_j is the jth frequency of the structure; ω_j^u is the upper limit for jth frequency and ω_j^l denotes its lower limit; L_k and U_k are the lower and upper limits of kth design variable, respectively. As it can be seen, the simple penalty function approach is used for constraint handling in this study. For each candidate solution, the penalty function is calculated as follows:

$$f_p(\{X\}) = \left(1 + \sum_{j=1}^{nc} \max(C^U(\{X\}), 0) + \max(C^L(\{X\}), 0)\right)^{\alpha} \quad (2)$$

where α is a constant value and nc and is the number of frequency constraints. The parameter α has a major effect on the algorithm's performance. At the initial stages of the optimization process, the value of this parameter should be small enough to explore the whole search space (exploration), while whatever the optimization process closes to the final stages, it should be large enough to provide more focus on the feasible solutions (exploitation). In this study, the value of α in Eq. (2) starts from 2 and linearly increases to 7 by lapse of the iteration (Kaveh and Zolghadr, 2014b) as follows:

$$\alpha = 2 + 5 \times \left(\frac{It}{It_{max}}\right) \quad (3)$$

where It and It_{max} are the current iteration number and maximum considered iterations, respectively.

3 OPTIMIZATION METHOD

3.1 Biogeography-Based Optimization

The Biogeography-based optimization (BBO) method inspired by biogeography science is a recently developed meta-heuristic algorithm which has been introduced by Simon (2008).The biogeography science describes the geographical distribution of biological organisms in nature. The overall framework of this algorithm is developed based on the probabilistic mathematical models of biogeography science. These mathematical models were developed by MacArthur and Wilson (1967) and explain how species migrate between the habitats. In the BBO algorithm, each habitat (H_i) is a solution candidate for the optimization problem and the position of each habitat (H_i) in an n-dimensional search space represented by Suitability Index Variables (SIVs), which is an n-dimensional vector. The quality of each habitat is measured by the Habitat Suitability Index (HSI), which is directly proportional to the fitness function value. Thus, the habitats with high HSI values are better solutions than the ones with low HSI values. The BBO algorithm consists of two main operators: migration and mutation.

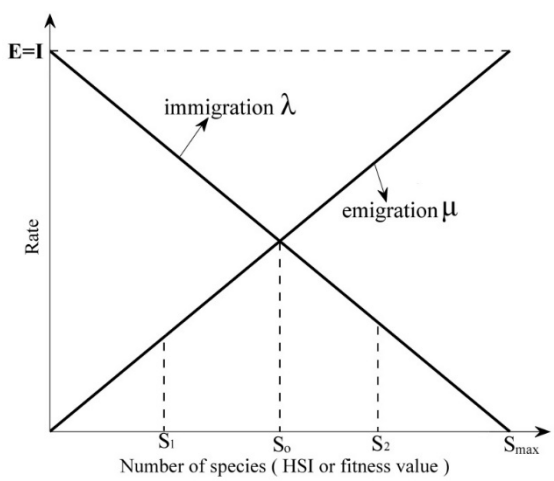

Figure 1: The simple linear migration model (E=I).

This algorithm utilizes migration operator as a powerful tool to share information between habitats in the solution space. So, it can be considered as an exploitation mechanism during the optimization process. The migration operator shares information between habitats based on immigration (λ_i) and emigration (μ_i) rates, probabilistically. Each habitat has its own immigration λ_i and emigration μ_i rates which are the functions of species in the habitat. For a given habitat, the immigration λ_i rate is inversely proportional to the HSI (fitness) value, while the emigration μ_i rate is directly proportional to HSI value. The habitats with high immigration rates (poor solutions) are more likely to accept information from the other habitats with high HSI values, while the habitats with low immigration rates (good solutions) share their information with other poor habitats with a high probability. The immigration and emigration rates are calculated for each habitat as follows (Simon, 2008):

$$\lambda_i = I\left(1 - \frac{K}{S_{max}}\right) \tag{4}$$

$$\mu_i = E\left(\frac{K}{S_{max}}\right) \tag{5}$$

where I is the maximum possible immigration rate; E is the maximum possible emigration rate; K is the number of species in the ith habitat; and S_{max} is the maximum number of species. These immigration and emigration rates are calculated based on the migration models. There are different migration models that can be utilized to calculate the immigration and emigration rates. Figure 1 shows the simple linear migration model for the case E=I. According to Figure 1, the habitats with a high HSI value tend to have a large number of species, while those with a low HSI have a small number of species (Simon, 2008). From Figure 1, it can be concluded that the habitat with few species (poor solution, low HSI) like S_1, has a low emigration rate and a high immigration rate. This means that, the habitat with low HSI tends to take information about the good habitats with the high probability, while the probability of sharing its information for other habitats is relatively low. On the other hand, the habitat which has more species (good solution, high HSI) like S_2, has a low immigration rate and a high emigration rate. Such habitats with high HSI values share their information with the other habitats with a high probability. By utilizing this mechanism, the migration operator of the BBO algorithm can achieve adequate exploitation ability between the habitats in the search space. For each variable of a given solution (H_i), the immigration λ_i rate decides whether or not to immigrate. If the immigration condition is satisfied, the migration procedure occurs between the immigrating and emigrating habitats as follows:

$$H_i(SIV) \leftarrow H_j(SIV) \tag{6}$$

Eq. (6) explains that one of the variables of ith habitat is replaced by a variable of jth habitat. Here, H_i and H_j are the immigrating and emigrating habitats, respectively. It is worth mentioning that the emigrating habitat (H_j) is selected based on the emigration rates (μ_i). The probability of selecting jth habitat as emigrating habitat is calculated as follow:

$$Prob\left(emigration\ from\ H_j\right) = \frac{\mu_j}{\sum_{i=1}^{N}\mu_i}, \text{ for j=1, 2, 3, …, } N_P \tag{7}$$

where N_P is the population size. Figure 2 demonstrates the details of the migration procedure in the BBO algorithm. Here, the roulette wheel selection technique is used to select emigrating habitat.

```
Habitat migration
Select H_i with probability α λ_i
 if H_i selected
   For k=1:N
    If rndreal(0,1)< λ_i
      Select H_j with probability α μ_i
      If H_j is selected
            Randomly select an SIV σ from H_j
            Replace a random SIV in H_i with σ
      end if
    end if
   end for
 end if
```

Note: N is the dimension of the search space.

Figure 2: The migration procedure of the BBO algorithm.

In most cases, it is possible that a meta-heuristic algorithm is trapped to the local optimum by lapse of the iteration. In order to escape from the local traps in the search space, the BBO algorithm utilizes a mutation operator. Mutation operator is a probabilistic operator that modifies a habitat's SIV randomly based on mutation rate ($pMutate$), which is related to the habitat's probability. The mutation rate ($pMutate$) for each habitat is calculated as follows:

$$pMutate = m_{max}\left(\frac{1-P_i}{P_{max}}\right) \tag{8}$$

where m_{max} is a user-defined parameter and $P_{max} = \max\{P_i\}$. More details about the calculation of P_{max} and P_i probabilities can be found in (Simon, 2008). Based on Eq. (8), a variable of each habitat mutates randomly in search space with a given probability. For a better explanation, the mutation operator of the BBO algorithm can be described as in Figure 3. In this study, for simplicity, the probability of performing mutation operator for the all habitats is set to 0.1 ($pMutate = 0.1$).

```
Habitat mutation
For i=1:N_H
   Select H_i(j) with probability pMutate
        If H_i(j) is selected
             Replace H_i(j) with randomly generated SIV
        end if
end for
```

Note: N_H is the number of habitats.

Figure 3: The mutation procedure of the BBO algorithm.

Another feature of the BBO algorithm is that the elite habitats with high HSI values are selected to keep and transfer from previous generation to the current one. Therefore, the *Keeprate* parameter is defined for this purpose. In this study, 20% (*Keeprate=0.2)* of habitats with high HSI values are selected to keep in each generation. It means that the 20% of elite habitats from the previous population are transferred to the current generation and combined with new habitats. Finally, the habitats with high HSI values are selected from the combined population of habitats to form a new population.

For a better explanation, Figure 4 shows the flowchart of the standard BBO algorithm.

3.2 Enhanced Biogeography-Based Optimization

As mentioned before, the standard BBO algorithm may not be successful in finding better solutions for some non-linear complicated optimization problems. The main reason for this issue is that the basic BBO algorithm employs simple migration and mutation operators during the optimization process. Such simple operators may lead to some disadvantages such as a low exploration ability and premature convergence. In a migration operator, the immigrating habitat is updated by simply replacing one of the SIV of emigrating habitat randomly, which often implies a rapid loss of diversity in the population. With the aim of achieving a better exploitation capability and providing efficient information sharing between the habitats, the new migration operator is proposed as follows:

$$\boldsymbol{H}_i(SIV) \longleftarrow \boldsymbol{H}_i(SIV) + \Phi\left(\boldsymbol{H}_j(SIV) - \boldsymbol{H}_i(SIV)\right) + \Phi\left(\boldsymbol{H}_j^{best}(SIV) - \boldsymbol{H}_i(SIV)\right) \tag{9}$$

where $\boldsymbol{H}_i(SIV)$ and $\boldsymbol{H}_j(SIV)$ are the immigrating and emigrating habitats, respectively, Φ is a random number uniformly generated between the 0 and 1, and $\boldsymbol{H}_j^{best}(SIV)$ denotes the best position experienced by the emigrating habitat. As it can be seen from Eq. (9), the new migration operator changes a variable of ith habitat by considering both current and best positions of the emigrating habitat. The proposed migration scheme has an important role in achieving an efficient exploitation ability.

On the other hand, the purely random mutation operator of the standard BBO algorithm may lead to revisiting non-productive regions of the search space, which leads to weak exploration ability, excessive computational efforts, and long computing time. Therefore, in order to enhance the exploration ability and eliminate the effect of the purely random mutation, following mutation operator is proposed:

$$\boldsymbol{H}_i(SIV) \longleftarrow \boldsymbol{H}_i(SIV) + N(0,1)\left(\frac{\boldsymbol{H}_{max}(SIV) - \boldsymbol{H}_{min}(SIV)}{It}\right),\ \mathrm{I_t}=1,2,3,\ldots,It_{max} \tag{10}$$

where $N(0,1)$ is a random number generated according to a standard normal distribution with mean zero and standard deviation equal to one; $\boldsymbol{H}_{max}(.)$ and $\boldsymbol{H}_{min}(.)$ are the upper and lower bounds of the search space, respectively; It and It_{max} are the current iteration number and the maximum number of iterations, respectively. As it can be seen from Eq. (10), the size of the search space considered for the mutation procedure decreases with respect to time. It is worth mentioning that, whenever the mutated position of a habitat goes beyond its lower or upper bound, the habitat will take the value of its corresponding lower or upper bound.

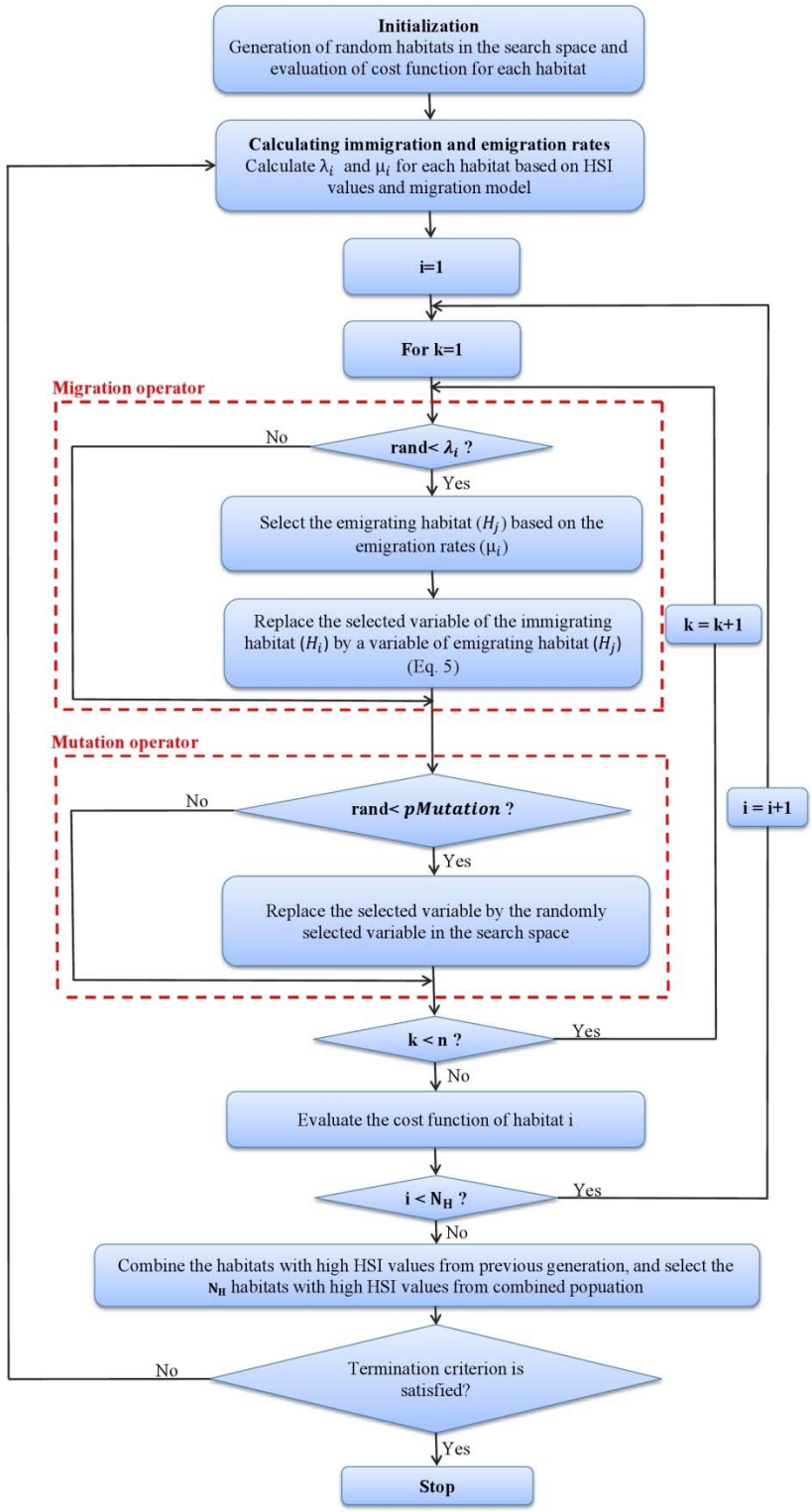

Figure 4: The flowchart of the standard BBO algorithm.

In order to better explain, the main steps of the proposed EBBO algorithm can be listed as below:
Step 1: Initialization

In the first step, the random habitats are generated in the search space as follows:

$$\boldsymbol{H}_i(SIV) = \boldsymbol{H}_{min}(SIV) + \Phi\ (\boldsymbol{H}_{max}(SIV) - \boldsymbol{H}_{min}(SIV)) \tag{11}$$

where Φ is the random number uniformly distributed between 0 and 1. Then, the value of HSI or cost function value is calculated for each habitat.
Step 2: Calculating immigration and emigration rates

In this step, the immigration λ_i and emigration μ_i rates are calculated for each habitat based on the migration model (Figure 1) and HSI values.
Step 3: Migration procedure

In the third step, the migration procedure is performed based on the immigration λ_i and emigration μ_i rates for each habitat by utilizing Eq. (9).
Step 4: Mutation procedure

After migration procedure, the variables of each habitat mutate with constant probability (*pMutation*) by Eq. (10).
Step 5: Evaluation of HSI values

In this step, the HSI values of the new generated habitats are computed.
Step 6: Formation of new population of habitats

A specific number of elite habitats from the previous population ($KeepRate \times N_P$) are transferred to the current generation and combined with the new habitats. Finally, the habitats with high HSI values are selected from the combined population of habitats to form a new population.
Step 7: Finish or redoing

Repeat from Steps 2–6 until the stopping criteria is met and output the best solution.

4 NUMERICAL EXAMPLES

In this section, four commonly used benchmark truss design examples with frequency constraints, including a 10bar planar truss, a simply supported 37-bar planar truss, a 120-bar dome truss and a 200-bar planar truss are examined to verify the performance of the proposed algorithm. In all design examples, the parameters used for both standard BBO and EBBO algorithms are set as follows: the population size is 50, and the *pMutation* is 0.1. The percentage of the selected habitats to keep is 20% of the population. Moreover, due to stochastic nature of EBBO algorithm and to demonstrate real behavior of the algorithm, 100 independent runs are considered for each design example, with each run starting from a random population. In addition, for the purpose of comparing standard BBO algorithm with the EBBO algorithm, 10 independent runs are also performed for the standard BBO algorithm and the results are reported. Moreover, the maximum number of analyses is defined as termination criterion of each run. For each design example, the maximum number of analyses is set as follows: 20,000 for the first two examples and 30,000 for the last two examples. The algorithms and finite element analyses are coded in Matlab software and implemented on Dell Vostro 1520 with Intel CoreDuo2 2.66 GHz processor and 4 GB RAM memory.

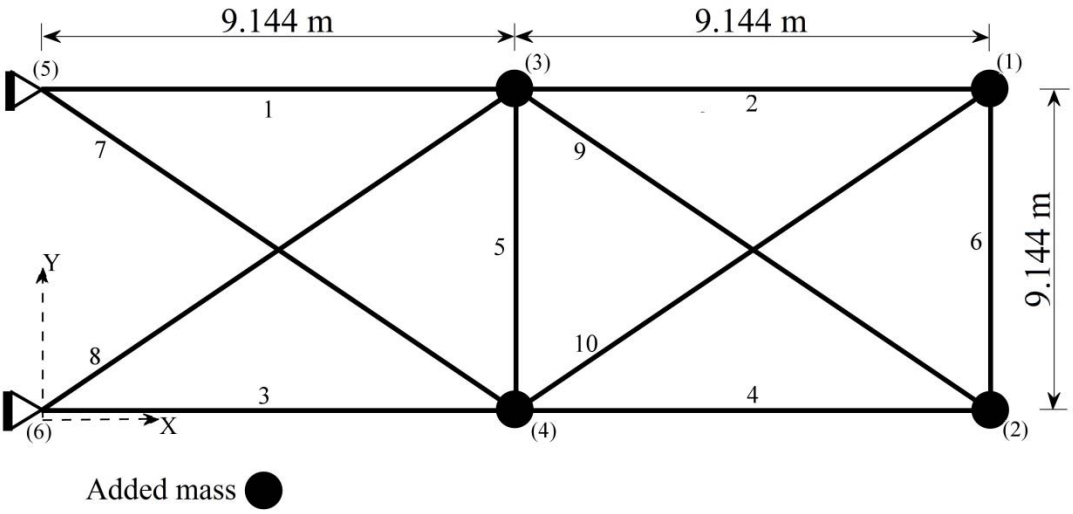

Figure 5:Schematic of 10-bar planar truss structure.

4.1 A 10-Bar Planar Truss Structure

The 10-bar planar truss structure with fixed configuration shown in Figure 5 is the first example. Young's modulus is 6.89×10^{10} N/m^2 and material density of truss members is 2770.0 kg/m^3. As seen in Figure 5, a non-structural mass of 454.0 kg is attached to all free nodes of the structure. The lower and upper bounds for the cross-sectional areas are specified as 0.645 cm^2 and 50 cm^2, respectively. The three natural frequency constraints are considered as: $\omega_1 \geq 7$ Hz, $\omega_2 \geq 15$ Hz, $\omega_3 \geq 20$ Hz. It is worth mentioning that, in some of the previous researches, the Young's modulus of the truss members is given as 6.98×10^{10} N/m^2. So, for a fair comparison, we considered two cases as follows: E= 6.89×10^{10} N/m^2 (Case 1) and E= 6.98×10^{10} N/m^2 (Case 2).

For Case 1, the optimum designs obtained through various methods are tabulated in Table 1, wherein the best design is ensured by the EBBO algorithm. From Table 1, it can be seen that the EBBO algorithm not only yields a better design than the SGA method, but it also requires significantly less structural analyses. However, the values of standard deviation and average weight are larger compared to the SGA method. In addition, Table 2 presents the frequencies of the structure obtained by various methods at the optimum designs. According to Table 2, it can be concluded that the designs reported by Sedaghati et al. (2002) and HRPSO violate the design constraints.

For Case 2, the optimization results obtained by different methods are listed in Table 3. Based on Table 3, it can be easily observed that the best, average and standard deviation obtained by the EBBO algorithm are better than the PSO, CSS, enhanced CSS, CSS-BBBC, and HRPSO methods. Moreover, although the value of standard deviation yielded by the proposed algorithm is larger than the SGA method, the EBBO algorithm finds lighter structural weight than this method. It is also noteworthy to mention that, the proposed algorithm requires less structural analyses than the SGA method to reach optimum solution. Furthermore, the frequencies evaluated at the optimum designs are listed in Table 4. It can be seen that the design yielded by the EBBO algorithm is feasible.

Design variables (cm^2)	Grandhi And Venkayya (1988)	Seda-ghati et al. (2002)	Wang et al. (2004)	Lingyun et al. (2005)	Kaveh And Zolghadr (2014a)	Kaveh And Javadi (2013)	Gonçalves et al. (2015)	Present work	
				NHPGA	DPSO	HRPSO	SGA	BBO	EBBO
A_1	36.584	38.245	32.456	42.234	35.944	35.54022	35.398	38.5883	35.71233
A_2	24.658	9.916	16.577	18.555	15.530	15.29310	15.112	16.3174	14.98558
A_3	36.584	38.619	32.456	38.851	35.285	35.78427	36.174	36.2167	35.61053
A_4	24.658	18.232	16.577	11.222	15.385	14.60570	14.762	12.8491	15.07165
A_5	4.167	4.419	2.115	4.783	0.648	0.64554	0.645	0.6498	0.64500
A_6	2.070	4.419	4.467	4.451	4.583	4.62572	4.620	4.9108	4.61214
A_7	27.032	20.097	22.810	21.049	23.610	24.77893	24.433	27.5541	23.94093
A_8	27.032	24.097	22.810	20.949	23.599	23.31005	23.723	21.3793	24.00576
A_9	10.346	13.890	17.490	10.257	13.135	12.48229	12.334	11.0164	12.38572
A_{10}	10.346	11.452	17.490	14.342	12.357	12.67468	12.602	12.1556	12.80152
Weight (kg)	594	537.01	553.8	542.75	532.39	532.11	532.11	535.76	532.07
Mean weight (kg)	N/A[a]	N/A	N/A	552.447	537.8	N/A	532.72	540.97	534.89
Standard Deviation (kg)	N/A	N/A	N/A	4.864	4.02	2.374	0.76	4.27	3.13
No. of analyses*	N/A	N/A	N/A	13,777	N/A	N/A	21,000	8500	16,200

* Number of analyses corresponding to the best result during 100 independent runs.

Table 1: Comparison of the optimal designs obtained by different methods for the 10-bar planar truss structure (Case 1).

Frequency No.	Grandhi and Venkayya (1988)	Seda-ghati et al. (2002)	Wang et al. (2004)	Lingyun et al. (2005)	Kaveh and Zolghadr (2014a)	Kaveh and Javadi (2013)	Gonçalves et al. (2015)	Present work	
				NHPGA	DPSO	HRPSO	SGA	BBO	EBBO
1	7.059	6.992	7.011	7.008	7.000	6.9999	7.0001	7.0456	7.0000
2	15.895	17.599	17.302	18.148	16.187	16.1752	16.1912	16.3072	16.1812
3	20.425	19.973	20.001	20.000	20.000	19.9999	20.0000	20.1299	20.0001
4	20.425	19.977	20.100	20.508	20.021	20.0060	20.0048	20.4485	20.0014
5	20.425	28. 173	30.869	27.797	28.470	28.5156	28.4758	27.7338	28.5019
6	30.189	31.029	32.666	31.281	29.243	28.9837	28.8965	29.0805	29.0158
7	54.286	47.628	48.282	48.304	48.769	48.5734	48.6102	48.9125	48.6089
8	56.546	52.292	52.306	53.306	51.389	51.0823	51.0822	51.8780	51.1237

Table 2: Comparison of the frequencies (Hz) obtained by different methods for the 10-bar planar truss structure (Case 1).

Design variables (cm^2)	Gomes (2011)	Kaveh and Zolghadr (2012)			Kaveh And Javadi (2013)	Gonçalves et al. (2015)	Present work	
	PSO	CSS	E-CSS[a]	CSS-BBBC	HRPSO	SGA	BBO	EBBO
A_1	37.712	38.811	39.569	35.274	34.793	34.282	35.1206	35.5816
A_2	9.959	9.031	16.740	15.463	15.245	15.062	14.6163	14.5615
A_3	40.265	37.099	34.361	32.110	35.562	36.205	34.4259	34.1122
A_4	16.788	18.479	12.994	14.065	13.836	14.566	14.6571	14.4837
A_5	11.576	4.479	0.645	0.645	0.646	0.645	0.7147	0.6450
A_6	3.955	4.205	4.802	4.880	4.583	4.554	4.7327	4.5901
A_7	25.308	20.842	26.182	24.046	25.535	24.120	23.4828	23.8959
A_8	21.613	23.023	21.260	24.340	22.300	23.172	24.5863	23.7897
A_9	11.576	13.763	11.766	13.343	11.614	12.080	14.8527	12.9001
A_{10}	11.186	11.414	11.392	13.543	13.072	12.641	10.6566	12.3566
Weight (kg)	537.98	531.95	529.25	529.09	524.88	524.70	527.66	524.64
Mean weight (kg)	540.89	536.39	538.53	N/A	N/A	525.68	533.58	527.00
Standard deviation (kg)	6.84	3.32	5.97	N/A	2.25	0.64	4.11	2.63
No. of analyses*	N/A	N/A	N/A	N/A	N/A	21,000	19,600	18,000

[a] Enhanced CSS; * Number of analyses corresponding to the best result during 100 independent runs.

Table 3: Comparison of the optimal designs obtained by different methods for the 10-bar planar truss structure (Case 2).

Frequency No.	Gomes (2011)	Kaveh and Zolghadr (2012)			Kaveh and Javadi (2013)	Gonçalves et al.(2015)	Present work	
	PSO	CSS	E-CSS	CSS-BBBC	HRPSO	SGA	BBO	EBBO
1	7.000	7.000	7.000	7.000	7.0000	7.0003	7.0006	7.0000
2	17.786	17.442	16.238	16.119	16.1686	16.2033	16.2650	16.1575
3	20.000	20.031	20.000	20.075	20.0015	20.0002	20.0472	20.0000
4	20.063	20.208	20.361	20.457	20.0050	20.0121	20.2079	20.0038
5	27.776	28.261	28.121	29.149	28.1466	28.4621	27.7244	28.6433
6	30.939	31.139	28.610	29.761	29.2724	28.9983	30.2389	29.1169
7	47.297	47.704	48.390	47.950	48.5235	48.6445	48.4195	48.3767
8	52.286	52.420	52.291	51.215	50.9950	51.1643	51.0860	50.9613

Table 4: Comparison of the frequencies (Hz) obtained by different methods for the 10-bar planar truss structure (Case 2).

Finally, the convergence characteristic of the BBO and EBBO algorithms for two cases are displayed in Figures 6 and 7. As it can be seen, the proposed algorithm reaches the near-optimum solution after 4000 analyses evaluated in 100 independent runs, while this value for standard BBO algorithm is about over 8000 analyses.

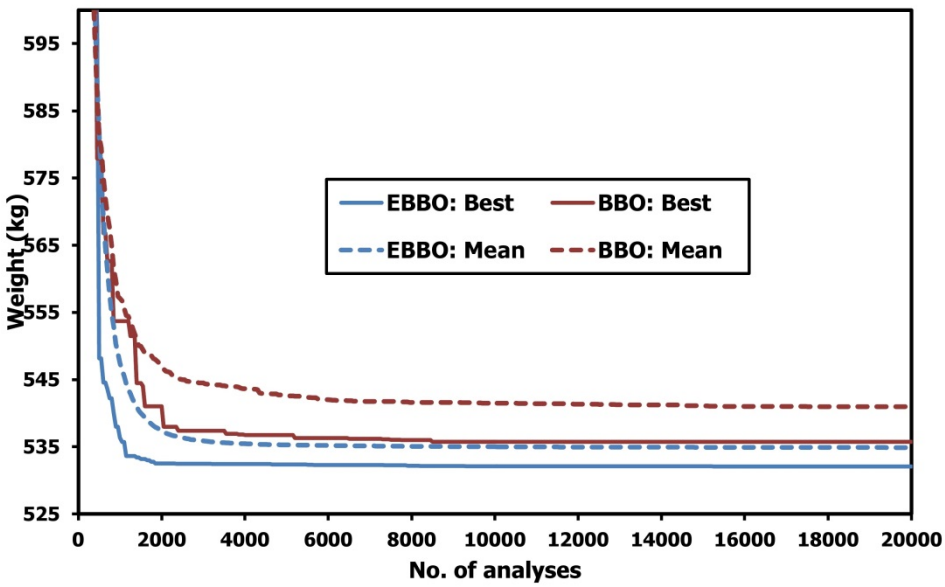

Figure 6: The Convergence diagrams of the EBBO and standard BBO algorithms for the 10-bar planar truss structure (Case 1).

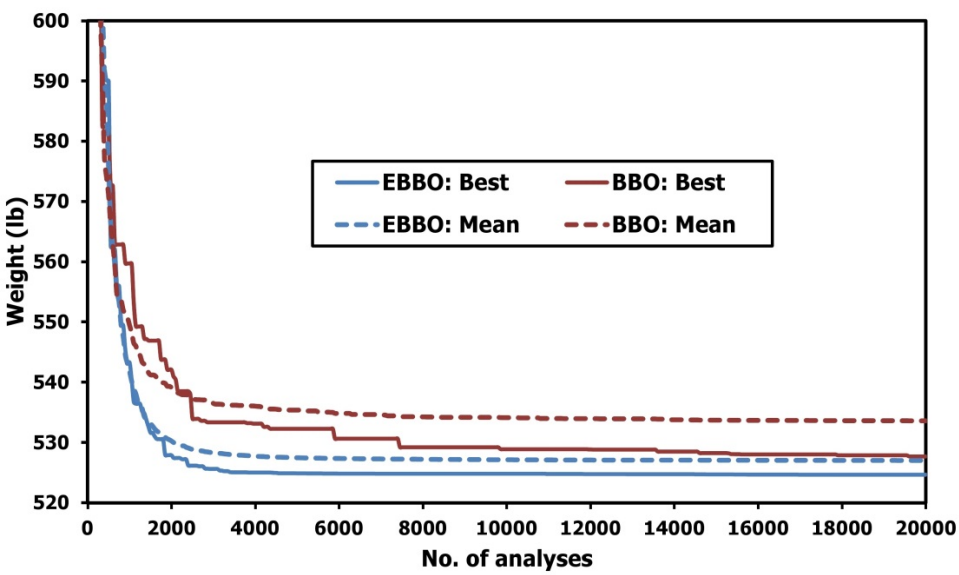

Figure 7: The Convergence diagrams of the EBBO and standard BBO algorithms for the 10-bar planar truss structure (Case 2).

4.2 A Simply Supported 37-Bar Planar Truss Structure

The second design example is the size and shape optimization of a simply supported 37-bar planar truss structure shown in Fig. 8. Young's modulus and material density of truss members are 2.1×10^{11} N/m^2 and 7800 kg/m^3, respectively. A non-structural mass of 10 kg is attached to free nodes at the lower chord of the structure. The constant rectangular cross-sectional areas of 4×10^{-3} m^2 are specified for all members of the lower chord and the cross-sectional areas of other members are considered as design variables. By considering geometrical symmetry, the y-coordinates of upper nodes are taken as layout variables and their vertical position can vary between ±1.5 m. Moreover, this structure is subject to the first three frequency constraints as follows: $\omega_1 \geq 20$ Hz, $\omega_2 \geq 40$ Hz, $\omega_3 \geq 60$ Hz.

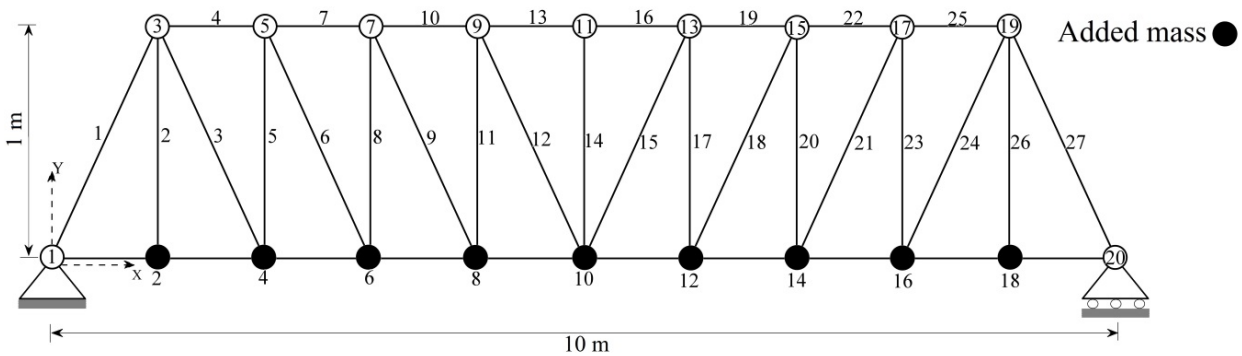

Figure 8: Schematic of the simply supported 37-bar planar truss structure.

The optimal designs obtained through various methods for this structure are tabulated in Table 5. From the results of comparisons given in Table 5, it can be concluded that the proposed algorithm is superior to the all other methods in solving this example by obtaining the lighter structural weight efficiently. The EBBO algorithm finds the minimum weight of 359.86 kg after 13,500 analyses, while the SGA method obtained the weight of 359.93 kg after 50,000 analyses. In addition, Table 5 also illustrates that: EBBO algorithm yields smaller standard deviation and mean weight than the HRPSO, OMGSA, DPSO, Enhanced CSS, CSS, and NHGA methods, and slightly larger than the values obtained by the SGA and FA methods. Moreover, the first five frequencies of the structure evaluated at the optimum design through various methods are listed in Table 6. As it can be seen, the design yielded by the EBBO algorithm is feasible and the design constraints are not violated.

Design variables	Wang et al. (2004)	Lingyun et al. (2005)	Gomes (2011)	Kaveh and Zolghadr (2011,2014a)			Khatibinia and Naseralavi (2014)	Kaveh and Javadi (2013)	Gonçalves et al. (2015)	Present work	
		NHGA	PSO	CSS	E-CSS	DPSO	OMGSA	HRPSO	SGA	BBO	EBBO
Y_3,Y_{19}	1.2086	1.1998	0.9637	0.8726	1.0289	0.9482	1.0064	1.07444	0.9670	0.9015	0.9573
Y_5,Y_{17}	1.5788	1.6553	1.3978	1.2129	1.3868	1.3439	1.4274	1.49568	1.3649	1.2273	1.3304
Y_7,Y_{15}	1.6719	1.9652	1.5929	1.3826	1.5893	1.5043	1.6171	1.73243	1.5388	1.4249	1.5144
Y_9,Y_{13}	1.7703	2.0737	1.8812	1.4706	1.6405	1.6350	1.7984	1.89449	1.6494	1.5431	1.6735
Y_{11}	1.8502	2.3050	2.0856	1.5683	1.6835	1.7182	1.8720	1.96970	1.7257	1.6336	1.7397
A_1,A_{27}	3.2508	2.8932	2.6797	2.9082	3.4484	2.6208	2.5017	2.85176	2.9114	2.5965	2.9399
A_2,A_{26}	1.2364	1.1201	1.1568	1.0212	1.5045	1.0397	1.0949	1.00000	1.0564	1.0172	1.0000
A_3,A_{24}	1.0000	1.0000	2.3476	1.0363	1.0039	1.0464	0.8891	1.83410	1.0004	1.1387	1.0000
A_4,A_{25}	2.5386	1.8655	1.7182	3.9147	2.5533	2.7163	2.5172	1.88766	2.4034	3.3397	2.5902
A_5,A_{23}	1.3714	1.5962	1.2751	1.0025	1.0868	1.0252	1.2119	1.06267	1.2688	1.0144	1.2003
A_6,A_{21}	1.3681	1.2642	1.4819	1.2167	1.3382	1.5081	1.3147	1.80266	1.2304	1.4436	1.1621
A_7,A_{22}	2.4290	1.8254	4.685	2.7146	3.1626	2.3750	2.1197	1.93387	2.7252	2.5162	2.6900
A_8,A_{20}	1.6522	2.0009	1.1246	1.2663	2.2664	1.4498	1.4223	1.24946	1.3238	1.6269	1.3599
A_9,A_{18}	1.8257	1.9526	2.1214	1.8006	1.2668	1.4499	1.5948	1.87404	1.5194	1.2487	1.5058
A_{10},A_{19}	2.3022	1.9705	3.86	4.0274	1.7518	2.5327	2.4784	1.95716	2.5593	3.0470	2.3627
A_{11},A_{17}	1.3103	1.8294	2.9817	1.3364	2.7789	1.2358	1.1896	1.24410	1.2390	1.3938	1.2500
A_{12},A_{15}	1.4067	1.2358	1.2021	1.0548	1.4209	1.3528	1.6461	1.77792	1.2506	1.2882	1.3544
A_{13},A_{16}	2.1896	1.4049	1.2563	2.8116	1.0100	2.9144	2.0878	1.80643	2.3692	3.3598	2.4491
A_{14}	1.0000	1.0000	3.3276	1.1702	2.2919	1.0085	0.5008	1.00000	1.0000	1.1207	1.0016
Weight (kg)	366.5	368.84	377.20	362.84	362.38	360.40	359.97	364.72	359.93	361.79	359.86
Mean weight (kg)	N/A	378.826	381.2	366.77	365.75	362.21	361.96	N/A	360.2	362.93	360.43
Standard Deviation (kg)	N/A	9.0325	4.26	3.742	3.461	1.68	1.868	5.776	0.26	1.02	0.44
No. of analyses*	N/A	14038	N/A	N/A	N/A	N/A	N/A	N/A	50,000	19,400	13,500

* Number of analyses corresponding to the best result during 100 independent runs.

Table 5: Comparison of the optimal designs obtained by different methods for the simply supported 37-bar planar truss structure; optimal nodal coordinates (m) and cross sectional areas (cm^2).

Frequency No.	Wang et al. (2004)	Lingyun et al. (2005)	Gomes (2011)	Kaveh and Zolghadr (2011,2014a)			Khatibinia and Naseralavi (2014)	Present work	
		NHGA	PSO	CSS	E-CSS	DPSO	OMGSA	BBO	EBBO
1	20.0850	20.0013	20.0001	20.0000	20.0028	20.0194	20.0220	20.04197	20.0005
2	42.0743	40.0305	40.0003	40.0693	40.0155	40.0113	40.0100	40.05697	40.0008
3	62.9383	60.0000	60.0001	60.6982	61.2798	60.0082	60.0490	60.07207	60.0039
4	74.4539	73.0444	73.0440	75.7339	78.1100	76.9896	76.4510	78.40251	76.3152
5	90.0576	89.8244	89.8240	97.6137	98.4100	97.2222	96.2970	97.99689	96.3553

Table 6: Comparison of the frequencies (Hz) obtained by different methods for the simply supported 37-bar planar truss structure.

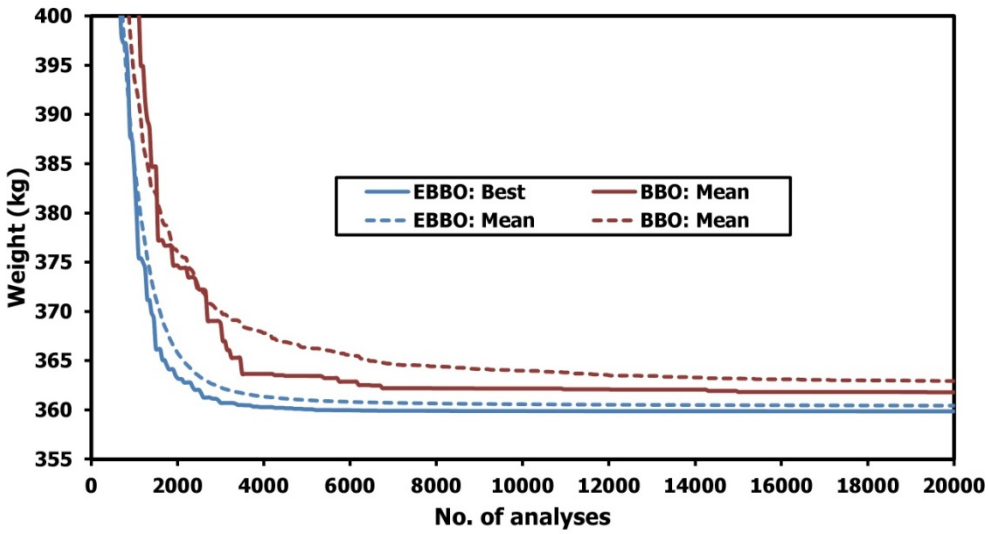

Figure 9: The Convergence diagrams of the EBBO and standard BBO algorithms for the simply supported 37-bar truss structure.

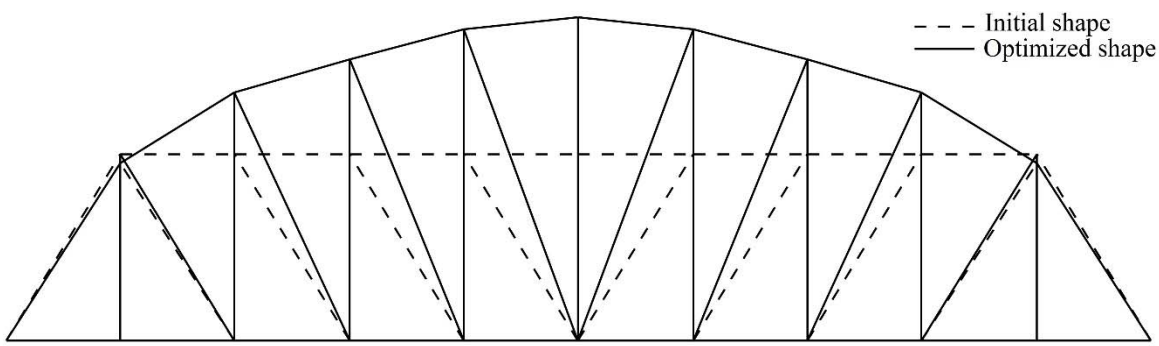

Figure 10: Comparison of the optimized shape with the initial configuration of the simply-supported planar 37-bar truss structure.

Figure 9 demonstrates convergence diagrams of the standard BBO and EBBO algorithms for the simply supported 37-bar planar truss structures. With regard to Figure 9, it is clear that the convergence speed of the EBBO algorithm is faster than that of the standard BBO algorithm. The EBBO algorithm reaches to the vicinity of final optimum solution after about 6000 analyses, while this value for the standard BBO algorithm is about 14,000 analyses. In addition, Figure 10 indicates the comparison of the initial and optimized shapes at the best design for this design example.

Element group	Kaveh and Zolghadr (2014a,2012)				Khatibinia and Naseralavi (2014)	Present work	
	CSS	CSS-BBBC	PSO	DPSO	OMGSA	BBO	EBBO
1	21.710	17.478	23.494	19.6070	20.2630	18.2999	19.8878
2	40.862	49.076	32.976	41.2900	39.2940	44.4985	39.8248
3	9.048	12.365	11.492	11.1360	9.9890	9.8161	10.5496
4	19.673	21.979	24.839	21.0250	20.5630	20.4079	21.0929
5	8.336	11.190	9.964	10.0600	9.6030	10.9003	9.4245
6	16.120	12.590	12.039	12.7580	11.7380	13.4254	11.6648
7	18.976	13.585	14.249	15.4140	15.8770	14.8123	15.1282
Weight (kg)	9204.51	9046.34	9171.93	8890.48	8724.97	8776.3	8711.95
Mean weight (kg)	N/A	N/A	9251.84	8895.99	8745.58	8916.9	8718.5
Standard deviation (kg)	N/A	N/A	89.38	4.26	1.18	128.63	7.15
No. of analyses*	N/A	N/A	N/A	N/A	N/A	29,850	6500

Table 7: Comparison of the optimal designs obtained by different methods for the 120-bar dome truss structure.

Frequency No.	Kaveh and Zolghadr (2014a,2012)				Khatibinia and Naseralavi (2014)	Present work	
	CSS	CSS-BBBC	PSO	DPSO	OMGSA	BBO	EBBO
1	9.002	9.000	9.0000	9.0001	9.002	9.0001	9.0000
2	11.002	11.007	11.0000	11.0007	11.003	11.0007	11.0000
3	11.006	11.018	11.0052	11.0053	11.003	11.0007	11.0002
4	11.015	11.026	11.0134	11.0129	11.007	11.0015	11.0002
5	11.045	11.048	11.0428	11.0471	11.076	11.0735	11.0657

*Number of analyses corresponding to the best result during 100 independent runs

Table 8: Comparison of the frequencies (Hz) obtained by different methods for the 120-bar dome truss structure.

4.3 A 120-Bar Dome Truss Structure

The third example is a 120-bar dome truss structure shown in Figure 11. The members of this structure are divided into 7 groups based on symmetry. The minimum and maximum cross-sectional areas for each group of members are 1 cm^2 and 129.3 cm^2, respectively. Young's modulus and material density of truss members are 2.1×10^{11} N/m^2 and 7971.810 kg/m^3, respectively. Non-structural masses are attached to all free nodes as follows: 3000 kg at node one, 500 kg at nodes 2 through 13 kg and 100 kg at the rest of the nodes. In addition, the structure is subject to frequency constraints as: $\omega_1 \geq 9$ Hz, $\omega_2 \geq 11$ Hz.

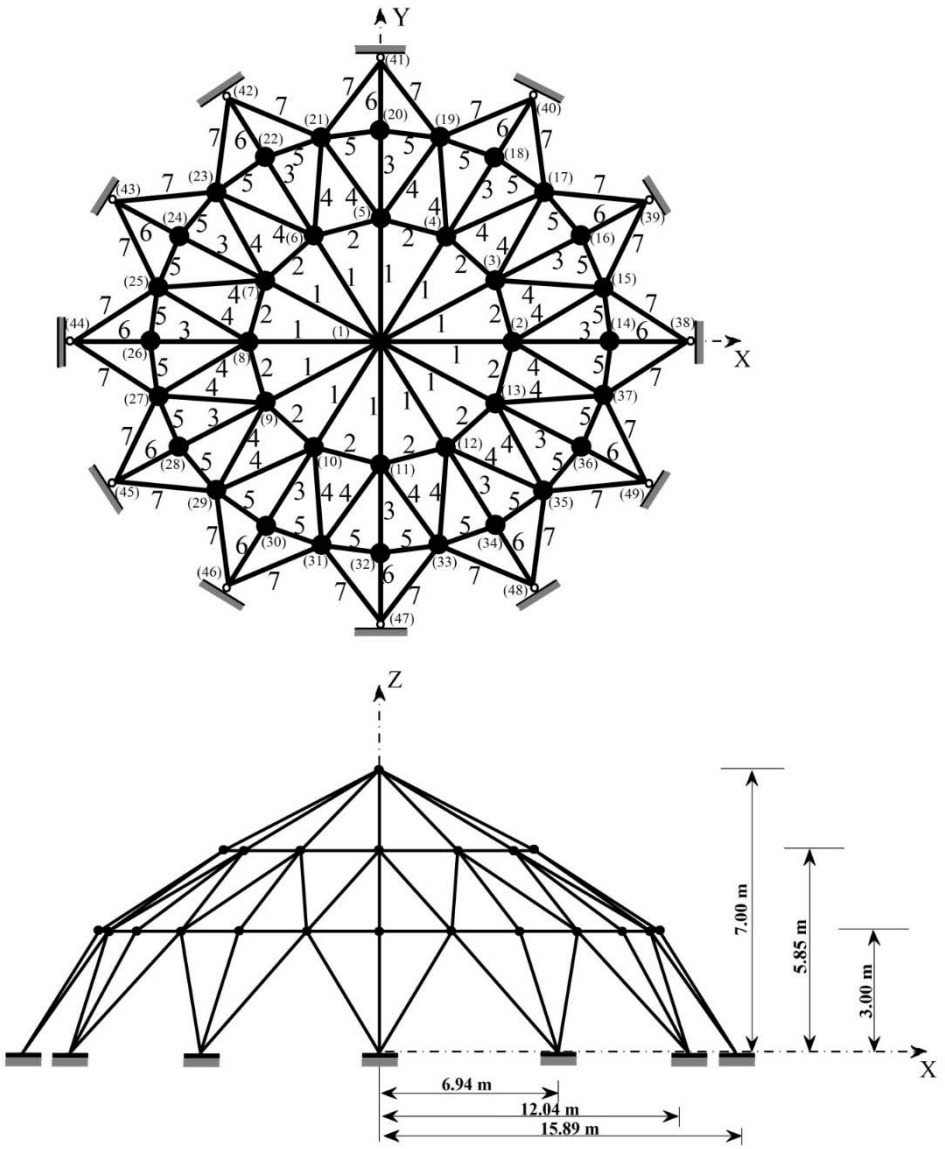

Figure 11: Schematic of the 120-bar dome truss structure: top and side views.

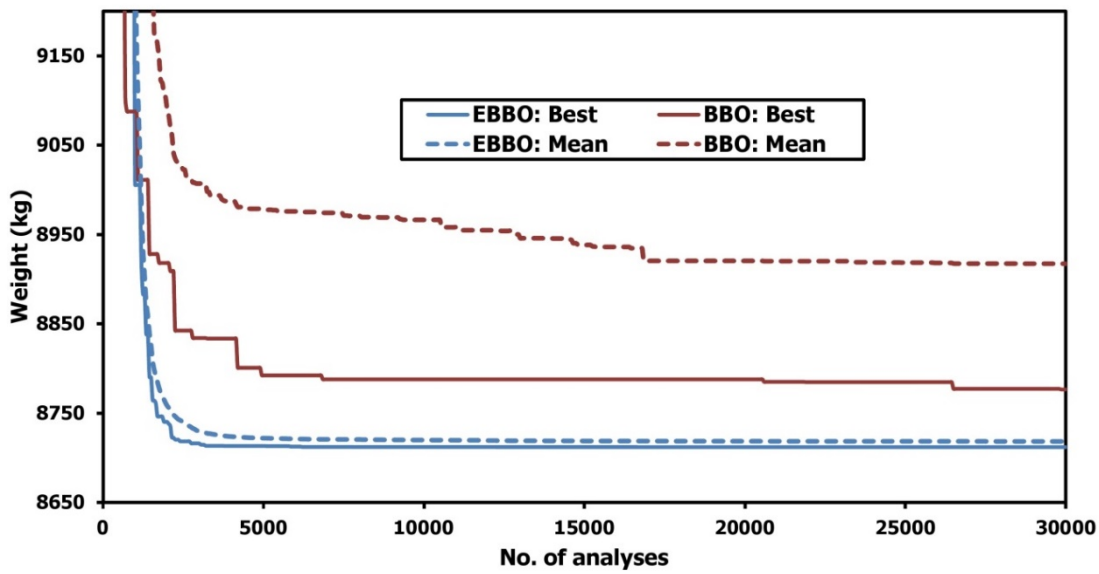

Figure 12: The Convergence diagrams of the EBBO and standard BBO algorithms for the 120-bar dome truss structure.

Group number	Members	Group number	Members
1	1, 2, 3, 4	15	102, 105, 108, 111, 114
2	5, 8, 11, 14, 17	16	82, 83, 85, 86, 88, 89, 91, 92, 103, 104, 106, 107, 109, 110, 112, 113
3	19, 20, 21, 22, 23, 24	17	115, 116, 117, 118
4	18, 25, 56, 63, 94, 101, 132, 139, 170, 177	18	119, 122, 125, 128, 131
5	26, 29, 32, 35, 38	19	133, 134, 135, 136, 137, 138
6	6, 7, 9, 10, 12, 13, 15, 16, 27, 28, 30, 31, 33, 34, 36, 37	20	140, 143, 146, 149, 152
7	39, 40, 41, 42	21	120, 121, 123, 124, 126, 127, 129, 130, 141, 142, 144, 145, 147, 148, 150, 151
8	43, 46, 49, 52, 55	22	153, 154, 155, 156
9	57, 58, 59, 60, 61, 62	23	157, 160, 163, 166, 169
10	64, 67, 70, 73, 76	24	171, 172, 173, 174, 175, 176
11	44, 45, 47, 48, 50, 51, 53, 54, 65, 66, 68, 69, 71, 72, 74, 75	25	178, 181, 184, 187, 190
12	77, 78, 79, 80	26	158, 159, 161, 162, 164, 165, 167, 168, 179, 180, 182, 183, 185, 186, 188, 189
13	81, 84, 87, 90, 93	27	191, 192, 193, 194
14	95, 96, 97, 98, 99, 100	28	195, 197, 198, 200
		29	196, 199

Table 9: Elements grouping for the 200-bar planar truss structure.

The obtained results through different optimization methods for this structure are summarized in Table 7. According to this table, one can observe that the design obtained by the EBBO algorithm is better than all the other methods. Although the value of standard deviation of the EBBO algorithm is larger than the values obtained by the OMGSA and DPSO methods, but the EBBO algorithm is more efficient than these methods in the term of the average of the results. In addition, it is important to note that the standard BBO algorithm obtained better results than the CSS, CSS-BBBC, PSO, and DPSO methods. However, it requires significantly more structural analyses than the EBBO algorithm. Moreover, the frequencies evaluated by different methods for the dome truss structure are listed in Table 8. As it can be seen, the values of the first two frequencies are very close to the allowable values.

Figure 12 illustrates the convergence diagrams of the standard BBO and EBBO algorithms for the 120-bar dome truss structure. As it can be observed, the convergence rate of the EBBO algorithm is considerably faster than the standard BBO algorithm. The proposed algorithm reaches to the vicinity of the final solution after about 5000 analyses evaluated in 100 independent runs without any abruption.

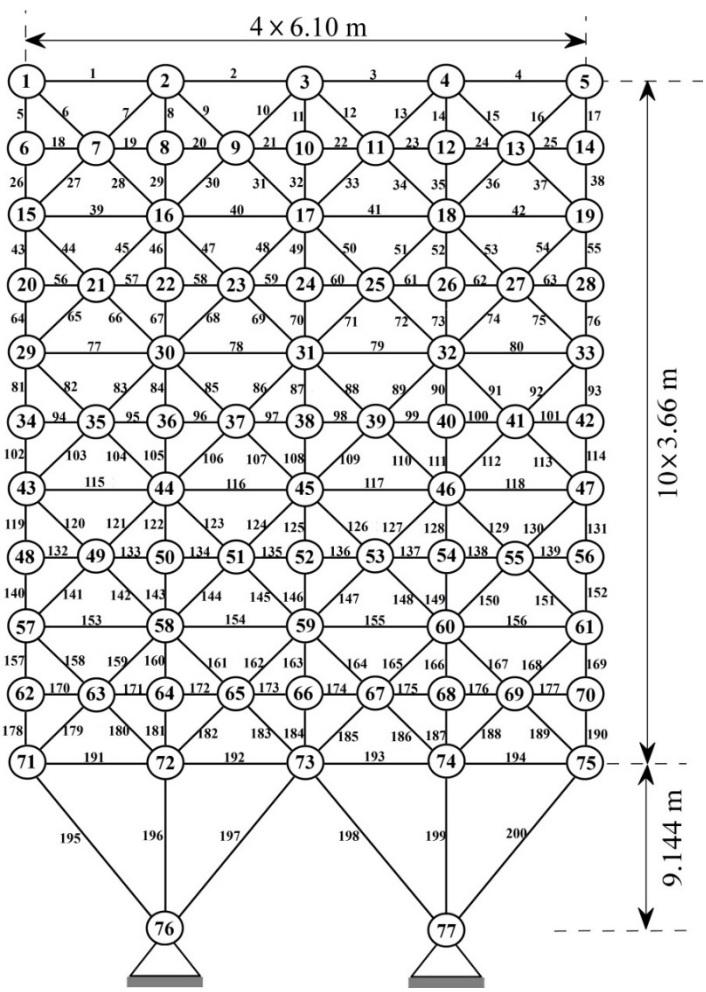

Figure 13: Schematic of the 200-bar planar truss structure.

Element group	Kaveh and Zolghadr (2012)		Khatibinia and Naseralavi (2014)	Present work	
	CSS	CSS-BBBC	OMGSA	BBO	EBBO
1	1.2439	0.2934	0.2890	0.1980	0.3059
2	1.1438	0.5561	0.4860	0.5928	0.4539
3	0.3769	0.2952	0.1000	1.6883	0.1000
4	0.1494	0.1970	0.1000	0.9960	0.1000
5	0.4835	0.8340	0.4990	1.4562	0.5210
6	0.8103	0.6455	0.8040	0.9733	0.8260
7	0.4364	0.1770	0.1030	0.7371	0.1000
8	1.4554	1.4796	1.3770	1.5266	1.4619
9	1.0103	0.4497	0.1000	0.1751	0.1001
10	2.1382	1.4556	1.5540	1.1536	1.5839
11	0.8583	1.2238	1.1510	1.2562	1.1426
12	1.2718	0.2739	0.1310	0.9819	0.1028
13	3.0807	1.9174	3.0280	3.0189	2.9913
14	0.2677	0.1170	0.1010	0.2562	0.1000
15	4.2403	3.5535	3.2610	1.8976	3.3607
16	2.0098	1.3360	1.6120	2.4537	1.5674
17	1.5956	0.6289	0.2090	1.1546	0.2825
18	6.2338	4.8335	5.0200	4.4126	5.1062
19	2.5793	0.6062	0.1330	0.5324	0.1000
20	3.0520	5.4393	5.4530	5.4785	5.4145
21	1.8121	1.8435	2.1130	4.0169	2.1388
22	1.2986	1.8435	0.7230	1.3088	0.7121
23	5.8810	8.1759	7.7240	6.1357	7.6374
24	0.2324	0.3209	0.1820	1.8785	0.1151
25	7.7536	10.9800	7.9710	8.1935	7.9160
26	2.6871	2.9489	2.9960	4.3817	2.8073
27	12.5094	10.5243	10.2060	11.5248	10.2844
28	29.5704	20.4271	20.6990	20.3022	21.2686
29	8.2910	19.0983	11.5550	12.1376	10.7450
Weight (kg)	2559.86	2298.61	2158.64	2539.85	2156.81
Mean weight (kg)	N/A	N/A	2167.53	2727.10	2157.80
Standard deviation (kg)	N/A	N/A	1.5860	85.18	1.25
No.of required analyses	N/A	N/A	N/A	29,100	16,500

Table 10: Comparison of the optimal designs obtained by different methods for the 200-bar planar truss structure.

4.4 A 200-Bar Planar Truss Structure

The last design example is a 200-bar planar truss structure shown in Figure 13. The Young's modulus is 2.1×10^{11} N/m^2 and the material density of truss members is 7860 kg/m^3. The minimum permitted cross-sectional area for the truss members is considered as 0.1cm^2. A non-structural mass of 100 kg is attached to the nodes at the top of the structure. In addition, the structure is subject to the first three frequency constraints as: $\omega_1 \geq 5$ Hz, $\omega_2 \geq 10$ Hz, $\omega_3 \geq 15$ Hz. The members of the structure are divided into 29 groups as shown in Table 9. This example has 29 design variables and it is considered a high dimensional optimization problem.

Table 10 compares the designs founded by the standard BBO and EBBO algorithms with other methods in the literature. With regard to the results given in Table 10, it is clear that the proposed EBBO algorithm obtained the lowest structural weight tan the CSS, CSS-BBBC, and OMGSA methods. In addition, the EBBO algorithm is more efficient than the OMGSA method in terms of average and standard deviation. Moreover, it can be seen from Table 10 that the standard BBO algorithm obtained better design than the CSS algorithm. Furthermore, the frequencies of the structure evaluated at the optimum designs are given in Table 11. Also, the design obtained by the EBBO algorithm is feasible, i.e., the constraints are not violated.

Frequency No.	Kaveh and Zolghadr (2012)		Khatibinia and Naseralavi (2014)	Present work	
	CSS	CSS-BBBC	OMGSA	BBO	EBBO
1	5.000	5.010	5.000	5.0067	5.0000
2	15.961	12.911	12.118	13.8669	12.2666
3	16.407	15.416	15.029	15.0755	15.0766
4	20.748	17.033	16.639	17.0058	16.7338
5	21.903	21.426	21.218	20.5140	21.4288
6	26.995	21.613	21.420	23.6846	21.5080

Table 11: Comparison of the frequencies (Hz) obtained by different methods for the 200-bar planar truss structure.

Figure 14 shows the convergence diagrams of the standard BBO and EBBO algorithms for this example. Again, it can be seen that the convergence rate of the EBBO algorithm is much faster than the standard BBO algorithm. Figure 14 reveals that the EBBO needs about 6000 analyses to reach near-optimum solutions evaluated in 100 independent runs.

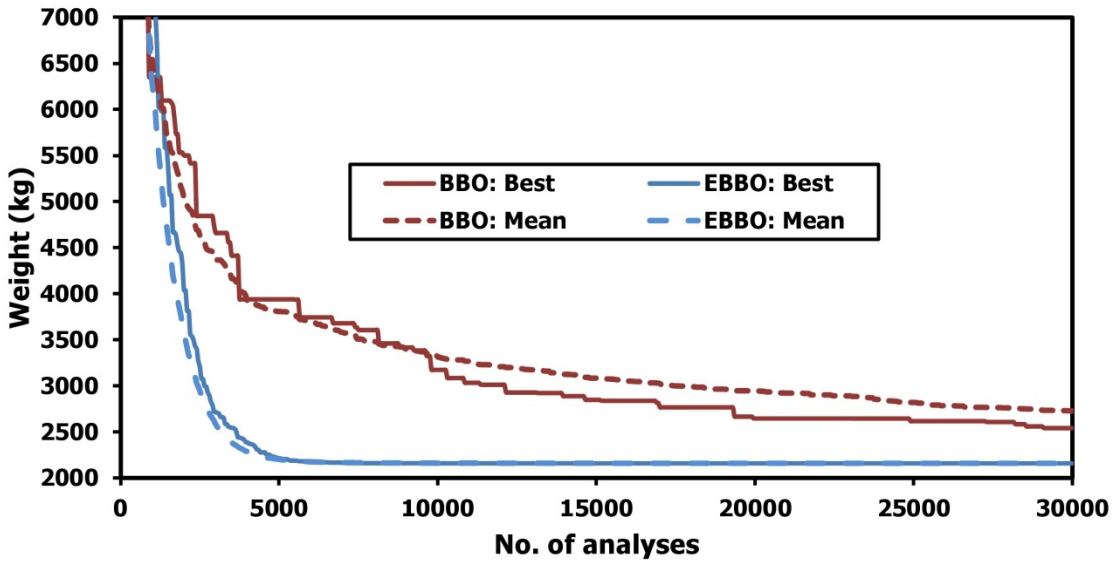

Figure 14: The Convergence diagrams of the EBBO and standard BBO algorithms for the 200-bar planar truss structure.

5 CONCLUSIONS

The Biogeography-Based Optimization (BBO) is a simple and recently introduced meta-heuristic optimization algorithm. The basic concepts and ideas of the method are inspired by the mathematical models in biogeography science and are based on migration behavior of species among habitats in the nature. The algorithm consists of two main operators: migration and mutation. In most cases, the standard BBO algorithm may fail to find the best solution. The main reason for this issue is that the basic BBO algorithm employs simple migration and mutation operators during the optimization process. Herein, an effective algorithm, called the Enhanced BBO (EBBO), has been developed to mitigate premature convergence problem of the standard BBO algorithm. In the proposed algorithm, to enhance the overall performance of the standard BBO algorithm, the new migration and mutation operators are proposed. The new migration and mutation operators improve the convergence properties of the BBO algorithm and enhance the algorithm's ability to further escape stagnation and premature convergence. To evaluate the performance of the proposed algorithm, four benchmark truss design examples with frequency constraints are investigated and the results are compared with those of the standard BBO algorithm and other methods in literature. The computational experiments show that the presented EBBO algorithm can get better solutions, and it is more efficient than the standard BBO algorithm on the size and shape optimization of truss structures problems with frequency constraints. Moreover, it can be stated that the proposed algorithm is straightforward and free of computational complexity.

References

Bhattacharya, A., Chattopadhyay, P., 2010. Biogeography-Based Optimization for Different Economic Load Dispatch Problems, IEEE Transactions on Power Systems. 25(2):1064–1077.

Boussaid, I., Chatterjee, A., Siarry, P., Ahmed-Nacer, M., 2012. Biogeography-based optimization for constrained optimization problems. Computers & Operations Research 39(12):3293–3304.

Eberhart, R.C., Kennedy, J., 1995. A new optimizer using particle swarm theory. Proceedings of the Sixth International Symposium on Micro Machine and Human Science, Nagoya, Japan.

Erol, O.K., Eksin, I., 2006. New optimization method: big bang-big crunch. Advances in Engineering Software 37:106–111.

Goldberg, D.E. 1989. Genetic Algorithms in Search Optimization and Machine Learning, Addison-Wesley, Boston.

Gomes, M.H., 2011. Truss optimization with dynamic constraints using a particle swarm algorithm, Expert Systems with Applications 38:957–968.

Goncalves, MS., Lopez, RH., Miguel, LFF., 2015. Search group algorithm: a new meta-heuristic method for the optimization of truss structures. Computers & Structures 153:165–184.

Grandhi, R.V. 1993. Structural optimization with frequency constraints—a review. AIAA Journal 31:2296–2303.

Jalili, S., Hosseinzadeh, Y., 2015. A cultural algorithm for optimal design of truss structures. Latin American Journal of Solids and Structures. 12:1721-1747.

Jalili, S., Hosseinzadeh, Y., Taghizadieh, N., 2015. A biogeography-based optimization for optimum discrete design of skeletal structures. Engineerng Optimization. DOI: 10.1080/0305215X.2015.1115028.

Kaveh A, Javadi, SM., 2013. Shape and sizing optimization of trusses with multiple frequency constraints using harmony search and ray optimizer for enhancing the particle swarm optimization algorithm. Acta Mechanica 225: 1595-1605.

Kaveh, A., Zolghadr, A., 2011. Shape and size optimization of truss structures with frequency constraints using enhanced charged system search algorithm. Asian Journal of Civil Engineering 12:487–509.

Kaveh, A., Zolghadr, A., 2012. Truss optimization with natural frequency constraints using a hybridized CSS–BBBC algorithm with trap recognition capability, Computers and Structures 102-103:14-27.

Kaveh, A., Zolghadr, A., 2014a. Democratic PSO for truss layout and size optimization with frequency constraints. Computers & Structures 130:102–103.

Kaveh, A., Zolghadr, A., 2014b. Comparison of nine meta-heuristic algorithms for optimal design of truss structures with frequency constraints. Advances in Engineering Software 76:9-30.

Kaveh, A.,Talatahari, S., 2010. A novel heuristic optimization method: charged system search. Acta Mechanica 213:267–286.

Khatibinia, M., Sadegh Naseralavi, S., 2014. Truss optimization on shape and sizing with frequency constraints based on orthogonal multi-gravitational search algorithm. Journal of Sound and Vibration. 333:6349–6369.

Lingyun, W., Mei, Z., Guangming, W., Guang, M., 2005. Truss optimization on shape and sizing with frequency constraints based on genetic algorithm. Computational Mechanics 25:361–368.

MacArthur, R., Wilson, E., 1967. The Theory of Biogeography, Princeton University Press; USA.

Miguel, LFF. 2013. Shape and size optimization of truss structures considering dynamic constraints through modern metaheuristic algorithms. Expert Systems with Applications 39:9458–9467.

Rashedi, E., Nezamabadi-pour, H., Saryazdi, S., 2009. GSA: a gravitational search algorithm. Information Science 179: 2232–2248.

Reynolds, R.G., 1999. Cultural Algorithms: Theory and Application. In D. Corne, M. Dorigo, and F. Glover, edi-tors, New Ideas in Optimization, pages 367–378. McGraw-Hill.

Sedaghati, R., Suleman, A., Tabarrok, B., 2002. Structural optimization with frequency constraints using finite element force method. AIAA Journal 40:382–388.

Simon, D. 2008. Biogeography-based optimization. IEEE Transactions on Evolutionary Computation 12:702–713.

Simon, D., Rarick, R., Ergezer, M., Du, D. 2011. Analytical and numerical comparisons of biogeography-based optimization and genetic algorithms. Information Sciences 181(7):1224–1248.

Singh, U., Kumar, H., Kamal, T., 2010. Design of Yagi-Uda Antenna Using Biogeography Based Optimization. IEEE Transactions on Antennas and Propagation. 58(10):3375–3379.

Wang, D., Zhang, W.H., Jiang, J.S., (2004). Truss optimization on shape and sizing with frequency constraints. AIAA Journal 42:1452–1456.